ELSEVIER

Marine and Petroleum Geology 20 (2003) 883–899

Marine and Petroleum Geology

www.elsevier.com/locate/marpetgeo

Constraining the efficiency of turbidity current generation from submarine debris flows and slides using laboratory experiments

David Mohrig[a,*], Jeffrey G. Marr[b]

[a]*Department of Earth, Atmospheric and Planetary Sciences, Massachusetts Institute of Technology, 77 Massachusetts Avenue, 54-814, Cambridge, MA 02139, USA*

[b]*Saint Anthony Falls Laboratory, University of Minnesota, Mississippi River at 3rd Avenue, Minneapolis, MN 55414, USA*

Received 4 September 2002; accepted 5 March 2003

Abstract

Results from a small set of laboratory experiments are presented here that help further constrain the processes governing the production of turbidity currents from impulsive failures of continental shelf and slope deposits. Three mechanisms by which sediment can be transferred from a parent debris flow to a less-dense turbidity current were observed and quantified. These mechanisms are grain-by-grain erosion of sediment from the leading edge of the parent flow, detachment of thin layers of shearing material from the head of the parent flow, and turbulent mixing at the head of the parent flow. Which transfer process dominates an experimental run depends on whether the large dynamic stresses focused on the head of the debris flow are sufficient to overcome a effective yield strength for the parent sediment + water mixture and on whether the dynamic stresses are sufficient to induce the turbulent flow of the parent mixture. Analysis of data from Marr et al. [Geol. Soc. Am. Bull. 113 (2001) 1377] and Mohrig et al. [Geol. Soc. Am. Bull. 110 (1998) 387] support the use of a shear strength to dynamic stress ratio in constraining necessary critical values for occurrence of the different production mechanisms. Direct sampling of turbidity currents using racks of vertically stacked siphons was used to measure both the quantity of sediment eroded from the heads of non-mixing parent flows and the distribution of particle sizes transported by the developing turbidity currents. Acoustic backscatter imaging was used to better resolve the internal boundary separating any turbulent mixing zone near the front of a flow from unmodified parent material.

Keywords: Turbidity currents; Debris flows; Submarine landslides

1. Introduction

Turbidity currents are recognized as being a primary mechanism through which sediment is distributed in deep-ocean environments. Advances in understanding the dynamics of these currents have come from: (1) the interpretation of erosional and depositional geometries preserved in outcrop and defined by acoustical imaging of the seafloor and subsurface; (2) the interpretation of sedimentary structures and textures preserved in turbidites; (3) direct measurement of individual flows via laboratory and rare natural experiments; and (4) theoretical modeling of the flow and sediment-transport mechanics for turbidity currents. Very little of this work has been specifically directed at understanding and quantifying the processes of turbidity-current production, even though this information is fundamental to predicting the frequency, size and character of the flows that build the seascape. We present here the results from a small set of laboratory experiments that place quantitative constraints on one particular style of turbidity-current generation, their evolution from the sudden failure and subsequent down-slope transport of a pre-existing continental shelf or slope deposit. In particular, we examine the processes controlling the transfer of sediment from a relatively dense submarine debris flow or slide (sediment:water about 50:50 by volume) to a relatively dilute turbidity current (sediment:water typically $\leq$10:90 by volume). These processes are explored as a function of the original composition of the dense parent phase and as a function of transport velocity of the dense parent flow. The experiments place constraints on the efficiency of sediment transfer from the parent flow to its affiliated turbidity current and document a systematic bias in size of the particles that are transferred.

* Corresponding author. Tel.: +1-617-253-9429; fax: +1-617-258-7401.
E-mail address: mohrig@mit.edu (D. Mohrig).

0264-8172/$ - see front matter © 2003 Elsevier Ltd. All rights reserved.
doi:10.1016/j.marpetgeo.2003.03.002

At least three different initiation mechanisms for turbidity currents exist: (1) sediment erosion from or partial transformation of impulsively triggered submarine slides, slumps or debris flows (e.g. Hampton, Lee, & Locat, 1996); (2) direct river underflows (i.e. hyperpycnal flows; Mulder & Syvitski, 1995); and (3) grain-by-grain retrogressive failure of very steep walls cut into pre-existing sand-rich deposits (Van den Berg, Van Gelder, & Mastbergen, 2002). In case 3 the dilative behavior of a sand-rich deposit precludes development of a disintegrative failure, allowing sediment to directly pass into a turbidity current without temporarily residing in a slide, slump or debris-flow phase (Hampton et al., 1996; Van den Berg et al., 2002). We present experimental results relevant to mechanism 1 only. The slides and debris flows acting as the parent material for this style of initiation are distinguished from each other based on the degree of internal deformation associated with their transport. Slides undergo minor deformation, with strain focusing on some small number of basal shear zones. Strain associated with most debris flows is penetrative. In our laboratory experiments we observed the entire spectrum of internal deformation from focused to distributed. In all cases the generation of turbidity currents from these experimental flows was a surface-related phenomenon involving the exchange of sediment across the interface separating the moving parent material from the surrounding clear water. This implies that the production process is not directly influenced by granular mass flow type (i.e. slide or debris flow) but rather depends on the response of the parent material to the dynamic stresses arising at the fronts or heads of the parent flows.

Submarine debris flows and turbidity currents bracket the wide range in sediment concentration constituting granular mass flows. Many debris flows contain so much sediment that the particles are nearly touching and their water component is interstitial, behaving as a pore fluid. The effective viscosity of this liquid is typically many times greater than that of ambient seawater because of the presence of a significant number of fine grains (silt + clay-size particles) suspended in the fluid (Iverson, 1997; Parsons, Whipple, & Simoni, 2001; Thomas, 1965). The increase in viscosity, together with high sediment concentrations, act to significantly hinder the motion of fluid around the grains and effectively combines the sediment and water so that for some period of time they move down slope as approximately a single phase. Turbidity currents, on the other hand, are relatively dilute mixtures of sediment and water in which most of the particles are suspended in the interiors of currents by the drag from the upward-directed motions of turbulent eddies. In our laboratory experiments it was straightforward to identify end-member cases of either type of granular mass flow. Considerable ambiguity in how to best categorize any particular flow arose as the sediment concentration in that flow approached transitional values of approximately 10–30% by volume.

Most original mixtures of sediment and water traversed our laboratory channel as debris flows. Large dynamic stresses acting on the front or head of each flow were responsible for the generation of any affiliated turbidity current. These stresses arose from accelerations associated with the deflection of ambient fluid by the debris flow from its path. Three styles of sediment transfer from a parent debris flow to a turbidity current were observed: (1) the grain-by-grain erosion of sediment from the surface of a flow and its subsequent ejection into the overlying water column (Figs. 1a and 2; Hampton, 1972; Marr, Harff, Shanmugam, & Parker, 2001; Mohrig, Whipple, Hondzo, Ellis, & Parker, 1998); (2) the shearing of thin layers of parent material from the head of a flow and its ejection into the overlying water column (Fig. 1b; Hampton, 1972; Marr et al., 2001); and (3) the turbulent mixing of ambient water into the head of a parent flow causing dilution and local transformation to a turbidity current (Fig. 1c; Allen, 1971; Hallworth, Phillips, Huppert, & Sparks, 1993; Marr et al., 2001; Morgenstern, 1967). The environmental conditions that predispose a remobilized sedimentary deposit to one style of current production versus the other will be discussed in the following sections.

Our experimental results address two central questions of turbidity-current initiation via the impulsive failures of sedimentary deposits: what volume fraction of sediment from the original dense flow is worked into an overriding turbidity current and to what degree is the original dense flow diluted through the ingestion of ambient seawater with movement down slope? The answers to these questions constrain the initial concentration of suspended sediment within a resulting turbidity current as well as the initial volume of the current. This information is necessary input data for almost all quantitative models of turbidity currents and therefore is prerequisite for many predictions regarding the role of turbidity currents in construction of the seascape.

2. Methodology

2.1. Experimental facility

The experiments were performed in a glass-walled tank that is 3 m high, 10 m long and 0.6 m wide (Fig. 3). Suspended within this tank is a rectangular channel with an inner width of 0.2 m. This inner channel is articulated with a break in slope at a distance of 5.7 m from the supply-tank gate. The upstream angle was set at 4.9° for Mohrig et al. (1998) and 6° for Marr (1999). The downstream slope angle was set at 1° in both sets of experiments. The bottom of the suspended channel was artificially roughened by a rubber mat with ridges extending from sidewall to sidewall so as to ensure that all flows developed finite shear layers near their bases. For every experiment the tank was filled with standing water into which a premixed slurry (sediment + water) was released impulsively from a supply tank through

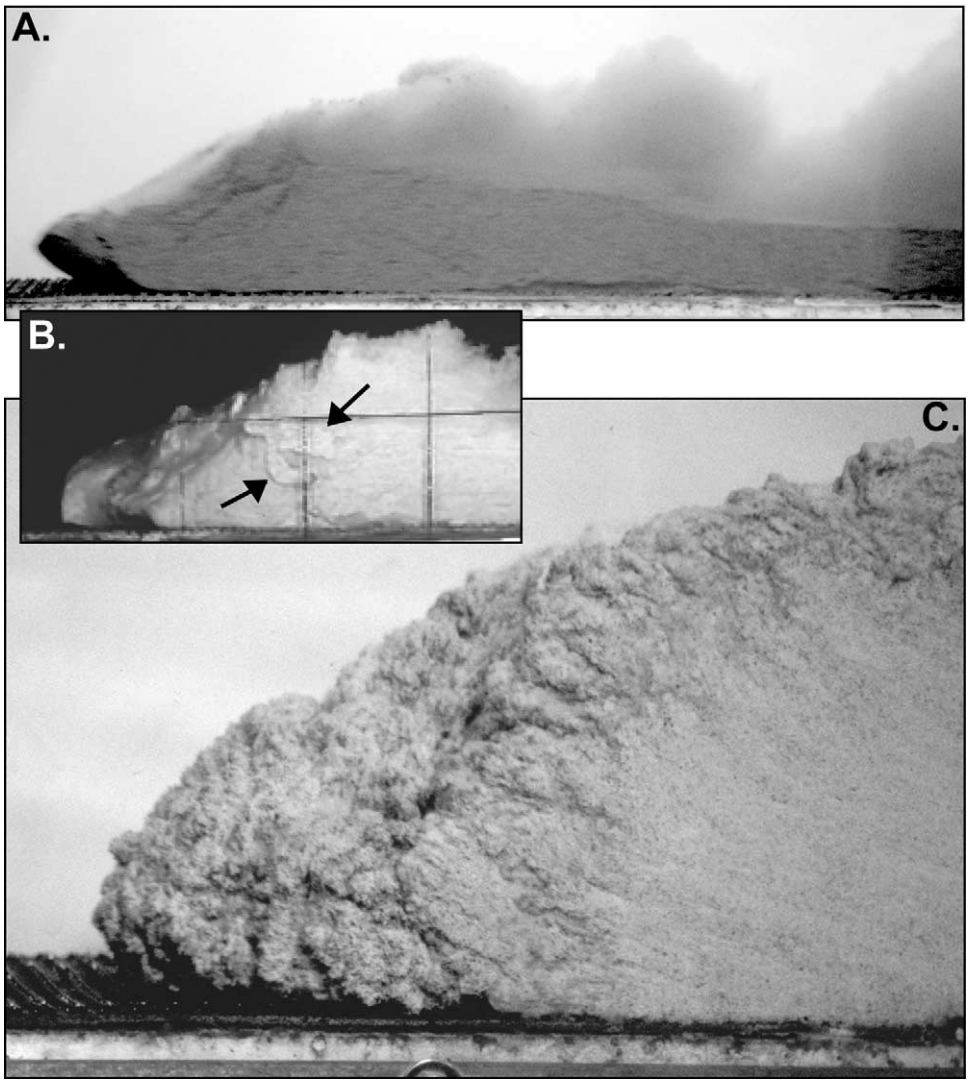

Fig. 1. (A) Sediment erosion from the head of a strongly coherent sediment-gravity flow (i.e. debris flow). Most of the material is eroded as individual grains, but a few multi-grain parcels of parent material are also observed. These 'clumps' of material tend to quickly settle out onto the top of the debris flow and are not worked into an overriding turbidity current. The horizontal field of view is 0.77 m. (B) Sediment erosion from the head of a moderately coherent sediment-gravity flow. The two arrows point to a thin layer of shearing parent material that has been shed from the head of the flow. The horizontal field of view is 0.40 m. (C) Turbulent mixing at the head of a weakly coherent sediment-gravity flow. Mixing of clear ambient water into the front of the flow is rapidly diluting the head and decreasing the volumetric concentration of sediment there from its initial value of 35%. The horizontal field of view is 0.37 m.

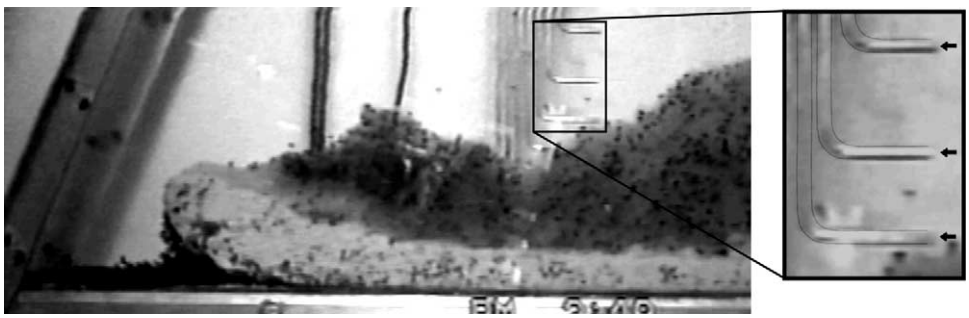

Fig. 2. Photo illustrating the siphoning system used to sample both composition and concentration of sediment suspended in turbidity currents overriding strongly to moderately coherent sediment-gravity flows (i.e. debris flows). Samples collected by a stacked rack of siphons resolve the vertical structure of studied turbidity currents. The horizontal field of view for the left-hand image is 0.68 m.

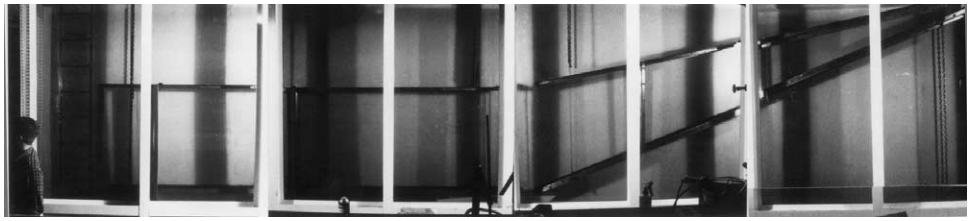

Fig. 3. Photograph of the experimental facility. An articulated inner channel is suspended within a tank that is 3 m high, 10 m long and 0.6 m wide. The supply tank from which concentrated mixtures of sediment and water are released to the inner channel is located just out of the field of view at the upper right-hand corner of the photo. A partial image of a lab assistant at the left-hand edge of the photo provides scale. The horizontal field of view is 9.7 m.

a rectangular aperture that was 0.20 m wide and rose about 0.03 m above the bed of the channel. Once opened, the gate to the supply tank remained so throughout the duration of each run. The volume of slurry released during each run was either 0.16 m^3 (Mohrig et al., 1998) or about 0.08 m^3 (Marr, 1999).

The motion of each debris flow and any affiliated turbidity current was recorded by multiple video cameras mounted in front of the glass sidewall to the tank. Videotaping of each experimental run continued until after the flows came to rest and formed deposits. Such parameters as head and body velocity, head and body flow thickness, the degree of turbulent mixing at the heads of flows, and deposit thickness were all determined through analysis of these tapes. Head velocities for the six experimental flows described in detail here are found in Table 1. Further descriptions of the setup for the experiments can be found in Mohrig et al. (1998) and Marr (1999).

2.2. Sampling of turbidity currents

Racks of vertically stacked siphons were used to sample the sediment concentration and grain size within turbidity currents generated through erosion of the heads of debris flows (Fig. 2). Each rack consisted of 5 siphons positioned 0.02, 0.05, 0.09 and 0.15 m above the lowermost siphon.

Table 1
Data for reported experimental flows

Run	Mud composition	δ_w	δ_s	Δ_w	Δ_s	γ_{sm}	γ_{ss}	U_h (m/s)
1	Silica	0.165	0.835	0.34	0.66	0.522	0.478	0.53
2	Silica	0.165	0.835	0.34	0.66	0.522	0.478	0.78
3	Kaolinite	0.300	0.700	0.53	0.47	0.286	0.714	0.74
4	Bentonite	0.300	0.700	0.53	0.47	0.021	0.979	0.82
5	Bentonite	0.300	0.700	0.53	0.47	0.032	0.968	0.68
6	Bentonite	0.300	0.700	0.53	0.47	0.043	0.957	0.53

Note: Here δ_w and δ_s are the mass fraction of water and sediment, respectively, so that $\delta_w + \delta_s = 1$; for comparison, Δ_w and Δ_s are the volume fraction of water and sediment, respectively, so that $\Delta_w + \Delta_s = 1$; γ_{sm} is the mass fraction of sediment consisting of mud (silt + clay-size particles) and γ_{ss} is the mass fraction of sediment consisting of sand, so that $\gamma_{sm} + \gamma_{ss} = 1$; and U_h is the head velocity for the parent flow. Runs 1 and 2 have the same composition as the flows reported in Mohrig et al. (1998). Runs 3, 4, 5 and 6 here are Runs 18, 2, 3 and 4 of Marr (1999), respectively.

This lowermost siphon was placed about 0.12 m above the bed of the channel to ensure that it did not in any way interfere with the debris flow as it passed beneath. An attempt was made to extract fluid from a turbidity current at a rate comparable to its average down-channel velocity. This approximate matching of rates reduced the likelihood for over- or under-sampling the sediment suspended within the system (Federal Interagency Sedimentation Project, 1941). Each siphon is made out of stainless steel and has an inner diameter of 4×10^{-3} m. Each siphon was connected to a collection bottle located outside of the tank by a short length of nylon tubing. Two turbidity currents were sampled over lengths of time of 24 s (Run 2, Table 1) or 48 s (Run 1, Table 1). These intervals of time were of sufficient duration to ensure that a meaningful average value was collected at each vertical position in the currents. The volume of current sampled by each siphon was about 0.2 l for Run 2 and about 0.4 l for Run 1.

2.3. Acoustical imaging of sediment-gravity flows

Measurements of acoustic reflectance collected with a reversible ultrasonic transducer were used to generate images constraining the extent to which ambient water was turbulently mixed into the heads of some debris flows (Marr, 1999). Employing such an imaging technique was necessary because sediment concentration in the diluted portions of these flows was still sufficiently high that it could not be distinguished from unmodified parent material by visual inspection alone. The submersible transducer had a footprint 2.54×10^{-2} m in diameter that was oriented orthogonal to the bed of the channel at a position 5 m down-slope from the supply-tank gate. It was aligned 1 m above a steel plate that was inset in the rubber matting roughening the channel base. This plate set up a large acoustic-impedance contract producing a reflection of ultrasonic energy that unambiguously defined the base of each flow. The transducer collected energy reflected by all interfaces of impedance contract at a time interval of about 0.06 s. This signal was fed directly to a personal computer. The chosen frequency for the acoustical pulse of 0.5 MHz provided a vertical resolution for each resulting reflection trace of about 3×10^{-3} m. Sequential traces collected at the fixed point as a flow passed beneath helped to resolve

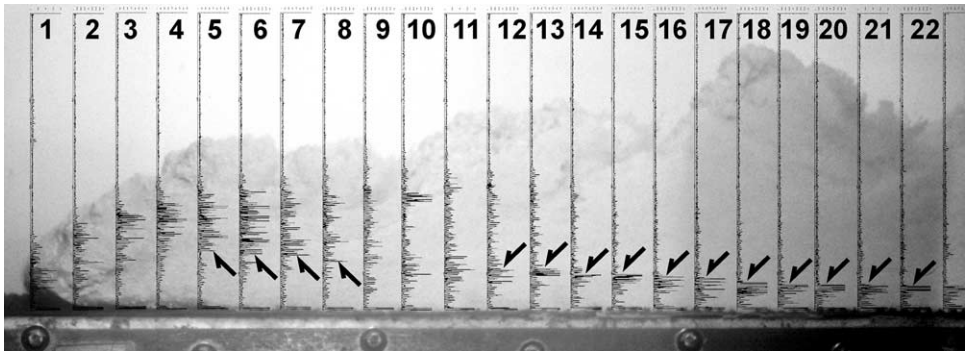

Fig. 4. Ultrasonic backscatter traces superimposed on a photograph of the corresponding sediment-gravity flow (Run 3, Table 1). Traces can be overlain on the photo because both the frequency of individual acoustical measurements and the mean velocity of the gravity flow at the data collection point are known. Individual traces are labeled from left to right. Arrows shown on individual traces mark the vertical position of the interface separating the overriding turbidity current from the underlying parent flow. The acoustical expression of this boundary changes in space because the reflectivity of the turbidity current changes with distance from the front of the flow (see text for details). Image length is 0.95 m.

the position of an internal boundary between a mixed zone and unaltered parent material if one occurred for that run.

Sequential traces of acoustic reflectance are overlain on a photograph of the corresponding sediment-gravity flow in Fig. 4 (Run 3, Table 1). The resulting image demonstrates the utility of the ultrasonic tool in separating the flow consisting of original parent material from the overlying turbidity current. Arrows on the traces in Fig. 4 mark this boundary between flows. The acoustical expression of this interface changes with distance from the front or head of the flow primarily because of a systematic spatial change in the reflectivity of the turbidity current. Near the front of the turbidity current an abrupt drop in average reflectivity defines its base (traces 3–8, Fig. 4). The high-amplitude reflections seen at this position within the overriding current are interpreted as stemming from two sources. One source is multiple surfaces of high impedance contrast associated with thin layers of parent material torn from the head of denser flow below and ejected into the developing current above. The other source is local density differences within the turbidity current associated with incomplete mixing of clear water from above into the turbulent sediment suspension (Fig. 4). By contrast, the relative lack of reflectivity within the underlying flow indicates approximately homogeneous properties for the unmodified parent material.

The systematic decrease in amplitude of reflections seen within the turbidity current from trace 5–16 (Fig. 4) is interpreted as caused by primarily two processes. The first process involves rapid removal of discrete layers of higher-density parent material from the turbidity current. This occurred either by the disintegration of ejected layers into constituent grains that were mixed into the current or by rapid settling of intact layers of parent material out of the current. Both cases removed numerous surfaces of high impedance contrast from the turbidity current. The second process is the continual dilution of the current by ongoing entrainment of clear water. Overall dilution steadily reduced the magnitude of any density contrast between the current and the clear water being mixed into it. This reduction in density contrast translated into smaller values of impedance contrast. Because of the strong spatial change in reflectivity of the turbidity current, its contact with the underlying parent flow is defined either by an abrupt change in average reflection amplitude with distance from the bed (e.g. traces 5–8, Fig. 4) or by a narrow band of high-amplitude reflections marking the top of one flow and the base of the other (e.g. traces 12–22, Fig. 4).

2.4. Composition of the parent material

The production of turbidity currents from subaqueous, granular mass flows is characterized here by results from six experimental runs (Table 1) possessing a wide range in composition of the parent material (i.e. the sediment + water mixture released from the supply tank). Parent materials varied in their water content, in their cumulative grain-size distribution (Fig. 5) and in the mineralogy of their clay-size particles (Table 1). Water contents used here were either 53% by volume (Runs 3, 4, 5 and 6) or 34% by

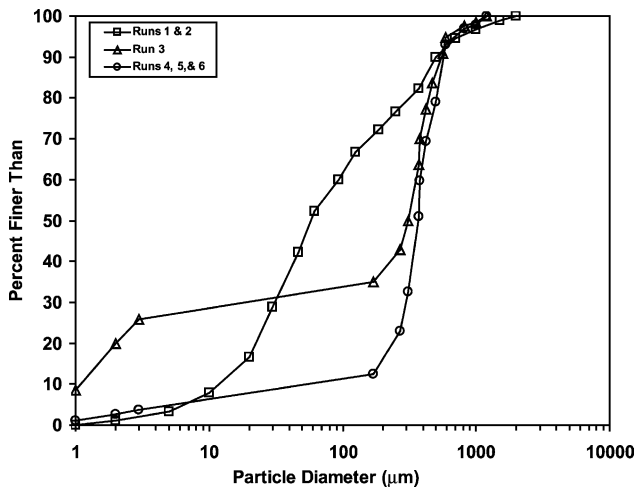

Fig. 5. Cumulative distributions of grain size for the three sediment mixtures reported in Table 1.

volume (Runs 1 and 2). This variability was primarily a reflection of the differences in the type of clay present in a flow. Bentonite used in Runs 4, 5 and 6 is a highly active clay mineral. The kaolinite used in Run 3 is a relatively inactive clay mineral and the silica used in Runs 1 and 2 is close to being chemically inert. As a result of these differences in charge activity, relatively large volume fractions of silica mud needed to be suspended within fresh water to produce liquid phases with effective viscosities comparable to those for relatively dilute mixtures of bentonite with water. Volume concentrations of kaolinite necessary to produce similarly viscous liquids were intermediate to those values for the bentonite and silica-mud mixtures (Table 1). For all laboratory experiments these liquid viscosities were sufficiently small to ensure that the parent material would flow down the channel following release from the supply tank and sufficiently large to ensure that the sand fraction did not completely settle through a flow and separate from the water plus mud (silt + clay) over the time scales for experimental runs (Marr et al., 2001; Mohrig et al., 1998; Shanmugam, 2000).

Mixtures of sediment and water released from the supply tank are intended to represent granular mass flows shortly following their generation via disintegrative failure of preexisting slope or shelf-edge deposits. Proper modeling of this initial condition requires the preparation of sediment and water mixtures that are consistent with natural prototypes. Particularly significant is the choice of water content for a given grain-size distribution and mineralogy. If the volume fraction of water is too large an experimental flow can rapidly segregate into a denser lower phase and a dilute upper phase by gravitational settling of particles that had been artificially suspended by mixing processes within the supply tank. An example of such collapsing flows are the experiments of Postma, Nemec, and Kleinspehn (1988) where the original mixtures of sediment and water separated from each other, over very short distances, into basal laminar layers made up of the coarser sand and gravel and overriding turbulent layers containing lower concentrations of the finer-grain sediment. The parent mixtures of sediment and water prepared by Postma et al. (1988) contained 60–65% water by volume. Turbidity currents made up of sediment entrained as the coarser grains settle downward through original mixtures, *fluidization transformations* as defined by Fisher (1983), are distinct from the currents we describe below. We did not investigate this style of turbidity-current generation because of uncertainty in how to compare the high water contents of rapidly collapsing experimental flows with the lower volume fractions of water present in many naturally occurring disintegrative failures of sedimentary deposits.

3. Coherency of the parent flows

In order for a dense, subaqueous parent flow to move down the channel it must deflect the ambient fluid it encounters from its path. These deflections are necessary because the permeability for the parent mixture is sufficiently small to preclude almost any ingestion of the surrounding water (see discussion in Mohrig et al., 1998). Accelerations associated with the deflection of the ambient fluid produce dynamic normal and shear stresses that act on the very front or head of a displacing flow. These stresses can be relatively large and can, for instance, exceed the weight per unit area of the dense flow itself (Mohrig et al., 1998). The stresses impact both the amount of sediment that is transferred from the parent flow to an associated turbidity current and the style of this transfer by impacting the character of the interface between the parent material and surrounding water at the leading edge of the flow. Marr et al. (2001) evaluated this interface in terms of the 'coherence' of a parent flow. Following their definition, coherence describes the degree of erosion, breakup, and turbulent mixing occurring at the head of the parent flow for given dynamic stresses. Strongly coherent flows refer to cases where the dynamic stresses acting on heads are not sufficient to induce the local development of laminar shearing layers within the parent material. In these cases the production of sediment for affiliated turbidity currents almost exclusively comes from the erosion of individual particles from the sharply defined, leading edge of the parent flow (Figs. 1a and 2). Moderately coherent parent flows define an increasing degree of head breakup that is characterized by reverse laminar flow of the parent material (e.g. Hampton, 1972). With this surficial shearing, thin layers of material can be detached from the heads and ejected into the overlying water column where many disintegrate within the developing turbidity currents (Fig. 1b). Finally, weakly coherent flows experience turbulent mixing of the parent material in their heads in response to the superimposed dynamic stresses (Fig. 1c). Clear water mixed into the head of the parent flow as a consequence of this turbulence expands the head and reduces its bulk density.

Hampton (1972) proposed that the change from what we refer to here as a strongly coherent flow to a moderately coherent flow takes place when the dynamic stresses acting on the head exceed the yield strength, τ_y, for the parent material. We have evaluated this proposal using the 28 experimental runs described in Mohrig et al. (1998) and Marr et al. (2001). Quantitative estimates of τ_y were measured in the laboratory for every parent material used in these runs (see Appendix A of Mohrig, Elverhøi, & Parker (1999) and Marr et al. (2001) for details). Measured values for τ_y ranged from 10 to 80 Pa. Dynamic stresses were scaled using the theoretical stagnation pressure $\tau_f = 1/2\rho U_h^2$, where ρ is the density of the ambient fluid and U_h is the velocity at which the front of the flow advances into quiescent water. Calculated values of stagnation pressure ranged from 8 to 763 Pa. Values of the ratio τ_y/τ_f for the 28 flows are presented in Fig. 6. These data show the transition

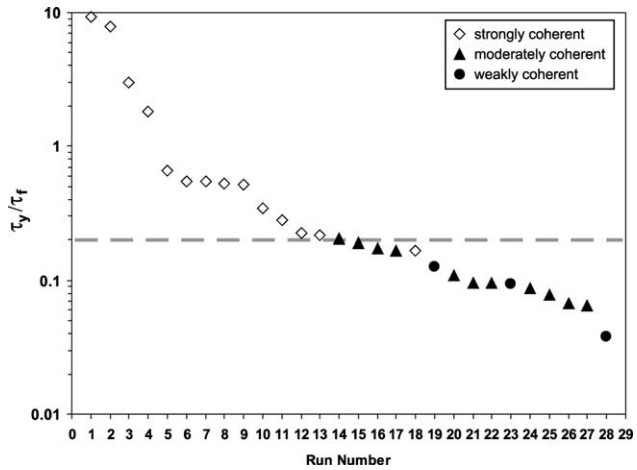

Fig. 6. Ratio of yield strength, τ_y, to dynamic stress, τ_f, for 28 experimental flows reported in Marr et al. (2001) and Mohrig et al. (1998). The 28 runs are sorted from left to right in descending value for τ_y/τ_f and show that the coherency for any particular parent flow is determined by the competition between the dynamic stresses that arise at its head and the strength of the parent material to resist deformation. For these experiments the transition from strongly to moderately coherent flows (Fig. 1a and b) occurred at a value for τ_y/τ_f of about 0.2, whereas the transition from moderately to weakly coherent flows (Fig. 1b and c) occurred at a somewhat lower value for τ_y/τ_f.

from strongly coherent to moderately coherent flows occurring over a relatively narrow range in value for the stress ratio. Specifically, the moderately coherent flows were found associated with values for $\tau_y/\tau_f < 0.2$. This result supports the original proposal by Hampton (1972) that a change in character of the interface between the front of a flow and the surrounding water occurs as the dynamic stresses acting on the head exceed the yield strength for the parent material.

The transition from moderately to weakly coherent flows is not resolved as well by the experimental data presented in Fig. 6. This lack of definition is at least partially a consequence of the small number of runs, only three, for which heads were identified as being weakly coherent. Because of this limitation we can only propose that this transition is associated with values for τ_y/τ_f somewhat smaller than the critical value of 0.2. A lower value for the stress ratio is consistent with an increase in the effective Reynolds number for the shearing layer parent material. Increasing Reynolds number forecasts its conversion from laminar to turbulent flow behavior. Analyses by Hanks (1963), Liu and Mei (1990), and Van Kessel and Kranenburg (1996) document this transition from laminar to turbulent flow for fluids with finite yield strengths. With the onset of turbulence the interface between the parent flow and surrounding water shifts from being discrete to gradational as clear water mixes into the front of the flow (Van Kessel & Kranenburg, 1996). The consequences of this changing interface on turbidity current generation are described in Section 4.

4. Processes of sediment transfer to turbidity currents from parent flows

4.1. Turbidity-current generation by strongly coherent parent flows

Strongly coherent parent flows are defined by the persistence of sharp interfaces separating the dense parent material from surrounding clear water at the leading edges of the flows. These interfaces remain sharp as flows travel down slope because dynamic stresses that act on the heads of the flows are not sufficient to cause development of surficial shearing layers within the parent material. In these cases the primary action of the dynamic stresses is to erode the heads grain-by-grain. Once particles are dislodged, they are ejected into the overlying water column where they are worked into a developing turbidity current (Fig. 7). Occasionally a coherent (i.e. non-deforming) chunk of parent material was torn from the front of the parent flow and ejected upward, but unlike the individual sediment grains these chunks rapidly settled through the developing turbidity current and came to rest on the upper surface of the parent flow. Shear at this upper interface separating the parent flow from its affiliated turbidity current was measured using nearly neutrally buoyant beads seeded within the ambient fluid. These beads show that shear at the interface rapidly decreases behind the head of a parent flow as the adjacent water is quickly accelerated to a velocity that is close to that of the parent flow. Very little shear along this upper interface meant that almost no sediment was transferred to an evolving turbidity current through the top of a strongly coherent parent flow.

In almost all of our experimental runs the heads of strongly coherent parent flows traveled at higher velocities than the affiliated turbidity currents. This difference in speed reflects the difference in the excess densities for the two styles flow that gravity can act on to move them down slope. The parent flows were substantially denser than the surrounding clear water while the currents, with their relatively low suspended-sediment concentrations, were only fractionally denser than the clear water. The driving force associated with the excess density for parent flows is not counterbalanced by a resisting force associated with their relatively high effective viscosities because the heads of these fast-moving flows were observed to hydroplane on very thin basal layers of lubricating water (Mohrig et al., 1998). In spite of their lower forward velocities, the turbidity currents were always more mobile than their source flows, peeling away from the tops of parent flows as they came to rest and continuing to advance down the slope (Fig. 8). In all of our experiments the velocities and bed stresses associated with these turbidity currents were not sufficient to erode sediment from the overlying parent-flow deposit. The depositional signature of the parent-flow/turbidity-current interaction was the construction of a very

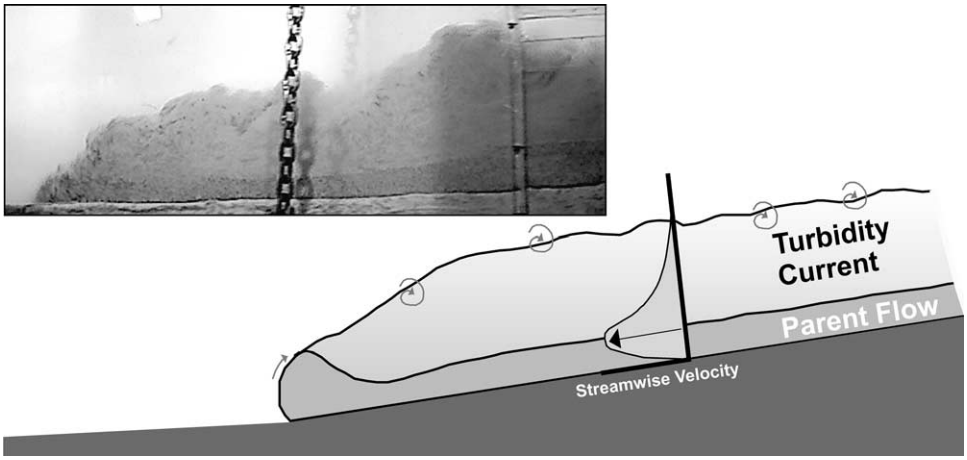

Fig. 7. The generation of a turbidity current from a strongly coherent debris flow. Sediment is eroded from the head of the debris flow via the large dynamic stresses that persist at this location. These stresses arise from acceleration of the ambient fluid up and over the head of the flow. Individual sediment grains are ejected into the overlying water, forming the turbidity current. There is very little shear observed at the debris-flow/turbidity-current interface and as a result very little sediment in transferred from a debris flow body to the turbidity current across its upper surface. The horizontal field of view for the complimentary inset photograph is 1.0 m.

thin turbidite that not only mantled the parent flow deposit, but extended in front of it as well.

4.2. Turbidity-current generation by moderately to weakly coherent parent flows

A change in the style and stability of the interface separating parent material from the surrounding clear water occurred as the dynamic stresses acting on the head of a flow exceeded its effective yield strength. These stresses were sufficient to cause the development of a layer of shearing parent material at the surface of the head of the flow. As long as the internal deformation within the shearing layer was laminar, the layer remained as a relatively thin veneer on the moving head. This was mostly because the material was continually lost from the layer as it was swept back from the leading edge of the parent flow and detached from the head on its leeward side (e.g. Hampton, 1972). Fig. 1b shows an example of thin layers being shed from the head of a moderately coherent flow. Following their ejection into the overlying water column these thin layers of parent material disintegrated to varying degrees into their constituent grains, which were in turn worked into the developing turbidity current. The remainders of detached layers rapidly settled onto the upper surface of the parent flow and were effectively reincorporated by the flow that shed them. Acoustical imaging of the moderately coherent flow shown in Fig. 4 (Run 3, Table 1) clearly revealed the short distance over which detached layers of parent material were either worked into the developing turbidity current or removed via settling. The high reflectivity associated with the occurrence of layers of unmodified parent material within the overriding turbidity current is limited to the first nine acoustic traces, a horizontal distance of only 0.3 m (Fig. 4).

The clear water/parent material interface at the leading edge of a moderately coherent flow was always relatively

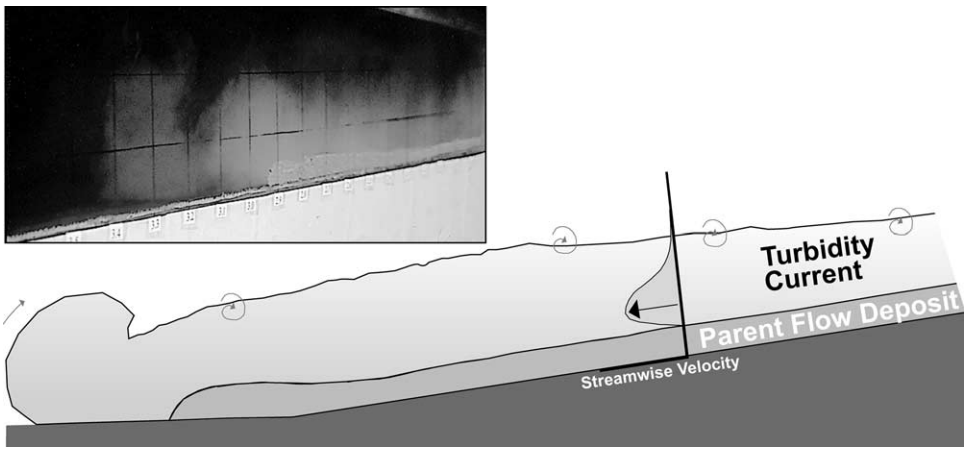

Fig. 8. As the strongly coherent debris flow comes to rest the turbidity current peels away from the top of the debris-flow deposit and continues advancing down slope. This current deposits a thin turbidite on top and in front of the debris-flow deposit. In all experiments, turbidity-current velocities were insufficient to erode sediment from the debris-flow deposit. The horizontal field of view for the complimentary inset photograph is 1.5 m.

sharp because the laminar character of deformation there precluded any fine-scale mixing of clear water into the head. This was not the case for a weakly coherent flow where the interface always appeared to be gradational. This change occurred when the dynamic stresses acting on the head of a flow were sufficient to drive its internal deformation from laminar to turbulent. Development of this turbulence resulted in the mixing of clear water into the deforming portion of the head and a dilution of the original sediment concentrations to levels more in line with those typically associated with turbidity currents. These are the only parent flows to undergo wholesale flow transformations. Turbidity currents that developed from grain plucking and/or shear-layer disintegration were essentially composed of sediment systematically eroded from the fronts of parent flows and this erosion did not involve fundamental change in the character of the parent flows themselves. In contrast, turbulent mixing rapidly transformed some forward portion of parent flows into turbidity currents. It was difficult to determine the extent of this transformation by visual inspection alone because sediment concentrations were everywhere sufficiently large to prevent even qualitative distinctions in its value. Marr (1999) discovered that transforming flows could be separated into their modified (turbulent) and unmodified (laminar) components by acquiring acoustical images of the experimental runs.

Fig. 9 contains the acoustical images from three runs. The image in Fig. 9a is of a strongly coherent parent flow and its affiliated turbidity current (Run 6, Table 1). This affiliated current was nearly transparent acoustically because of its very low suspended-sediment concentration, a concentration that was largely set by a low rate of sediment erosion from the head of the parent flow. Turbulent mixing was observed at the heads of the weakly coherent flows imaged in Fig. 9b and c (Runs 5 and 4, Table 1). Sequential acoustic traces mark out the distance over which parent material appears to have been modified via mixing with clear water. In Fig. 9b the unambiguous first occurrence of a sharp boundary separating

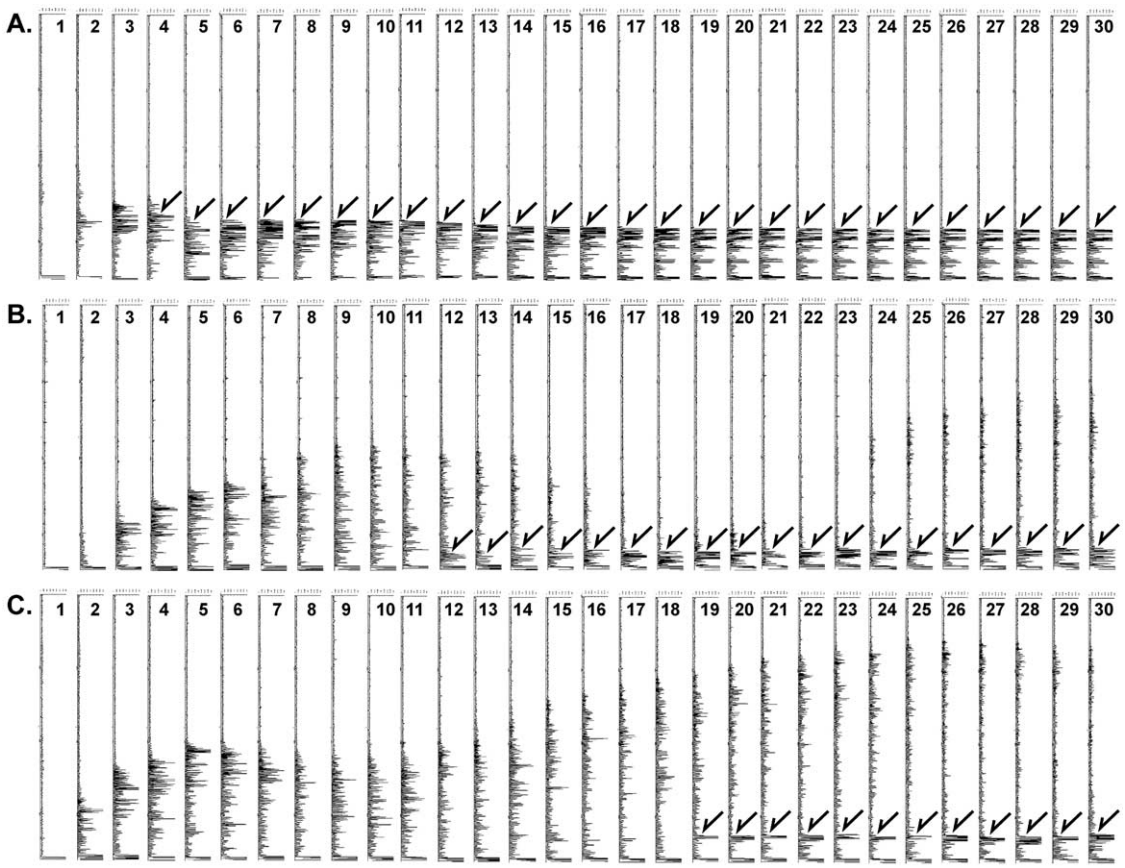

Fig. 9. Acoustic backscatter images for three subaqueous parent flows (Marr, 1999). These profiles are constructed by spatially aligning consecutive backscatter traces (see Fig. 4). Individual traces are labeled from left to right. Arrows shown on individual traces mark the vertical position of the interface separating the overriding turbidity current from the underlying flow made up of relatively unmodified parent material. (a) Backscatter image of a strongly coherent parent flow with no mixing of ambient water into its head (Run 6, Table 1). The dilute turbidity current that overrides this debris flow is not seen using the ultrasonic tool. Image length is 1.1 m. (b) Backscatter image of a parent flow with a turbulently mixing head followed by a laminar flowing body (Run 5, Table 1). Unmodified parent material constituting the body of the flow first appears on trace 12. Suspended-sediment concentrations within the turbidity current overriding this flow are sufficient for its acoustical resolution. Image length is 1.3 m. (c) Spatial change from turbulently mixing head to unmodified core in Run 4 (Table 1). First appearance of a possible dense core is seen at trace 14. Unmodified parent material is interpreted to arrive at trace 19. Traces 14–18 record the presence of a basal core that might be transitional to the fully mixed head of the flow and its unaltered body. Image length is 1.6 m.

the turbidity current above from unmodified parent material below is shown by an arrow on trace 12. In front of this position the turbulent mixing process disrupted any sharp interface between an overriding and underlying flow and replaced it with a more smoothly varying gradient in sediment concentration. Traces 1–11, taken together, do not record a spatial structure in reflectivity characteristic of the front of a turbidity current overriding unmodified parent material (see Section 2.3). The same is true for the traces 1–18 in Fig. 9c. This lack of any systematic vertical structure in the reflectivity is consistent with development of a gradational boundary by the mixing of clear water directly into the parent material.

In Fig. 9b the first occurrence of parent material that was apparently unmodified by mixing is at a distance of about 0.5 m from the very front of the flow. This distance was even greater for Run 4 (Fig. 9c, Table 1). For this run the first occurrence of parent material unmodified by mixing is marked by trace 19, a distance of about 1.0 m from the very front of the flow. Transformations associated with both of these weakly coherent flows (Fig. 9b and c) were clearly focused at their fronts where the dynamic stresses acting on them were large.

5. Sediment concentrations and grain sizes in affiliated turbidity currents

Determining exactly how much sediment was transferred from a parent flow and into an affiliated turbidity current required direct sampling using the siphoning system (Fig. 2). Such measurements were collected for Runs 1 and 2 (Table 1). Parent flow 1 was observed to be transitional, between strongly and moderately coherent, while flow 2 was moderately coherent. The turbulent mixing of clear water into the parent flow was not observed in either case. This meant that sediment constituting each turbidity current was solely derived from erosion of the head of its parent flow. Siphoned samples were used to determine how much sediment was eroded, how this sediment was distributed vertically within a current, and its grain size.

The concentration for suspended sediment was easily calculated for each siphoned sample of current by first weighing the water and sediment components and then converting these masses to volumes using densities for water and sediment of 1000 and 2650 kg/m^3, respectively. Choosing the appropriate density for the sediment in Runs 1 and 2 was straightforward because these flows were composed of quartz sand and silt and silica flour. Resulting sediment concentrations for the two currents are plotted in Fig. 10 as a function of distance from the bed of the channel. The data show that a five-siphon system adequately characterized the structure of the profile in the interior of each current. However, similar data could not be collected from the bottommost portion of each current. Siphons placed at these elevations clearly interacted with the heads of parent flows as they past by, calling into question the accuracy of any sample collected there. Basal concentrations for the currents could then only be estimated by extrapolating from each five-point data set. Our confidence

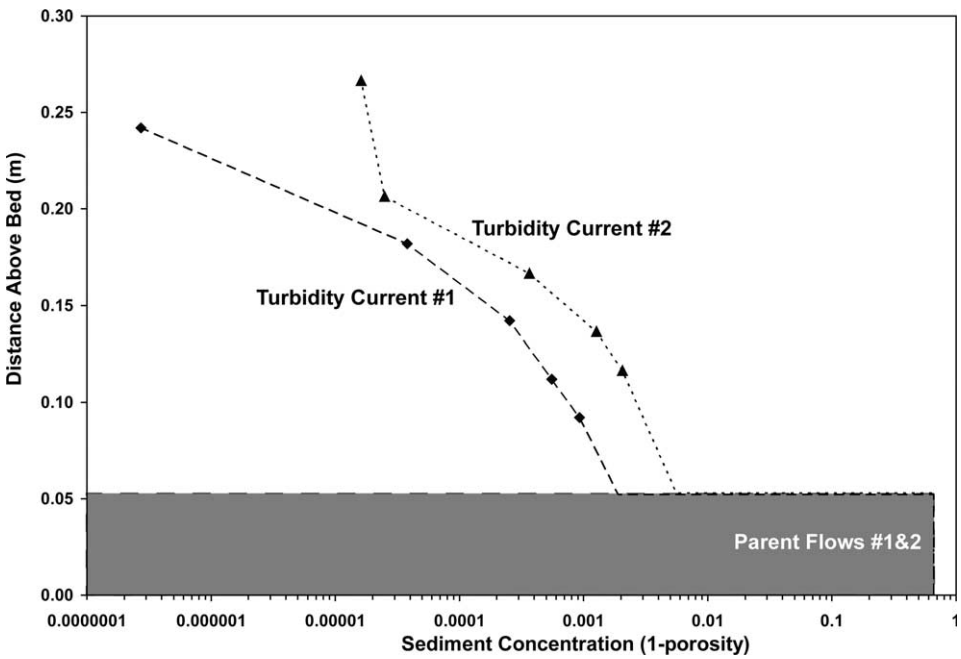

Fig. 10. Measured suspended-sediment profiles for the turbidity currents generated during Runs 1 and 2 (Table 1). Each symbol marks the vertical position of a sampling siphon in a rack located 2 m down-channel from the supply-tank gate (Fig. 3). The difference in bulk concentration between the two currents is interpreted to be the consequence of different head velocities for the parent debris flows. The measured concentration of the parent material is also on the plot and the shaded area defines the average debris-flow thickness. Notice the two orders of magnitude drop in sediment concentration at the debris-flow/turbidity-current interface.

in the basal value for each current is relatively high because the trends from which they were projected are robust. In Fig. 10 these basal values are shown at an elevation 0.05 m above the bed of the channel. This elevation is equal to the thickness of the body for each parent flow as measured from video collected during the experimental runs. Estimated values for the basal concentrations of currents 1 and 2 are 1.9×10^{-3} and 5.6×10^{-3}, respectively. The calculated average values of suspended-sediment concentration for currents 1 and 2 are 4.8×10^{-4} and 1.5×10^{-3}, respectively. These values are substantially less than the measured sediment concentration for the parent material of 6.6×10^{-1} (Table 1). This value is also plotted in Fig. 10, highlighting the step-function change in sediment concentration at the interface between the parent flow and the overriding turbidity current.

The sediment samples collected from the turbidity currents were noticeably finer grained than the distribution of sizes present in the parent material (Fig. 5). Sand was recovered from only the two lower siphons for both currents. Samples from the three upper siphons were exclusively mud (silt + clay-size particles). Only the samples from turbidity current 2 (Fig. 10) contained enough sand to warrant particle-size analysis. Grain-size distributions for the samples from the two lowermost siphons, along with the size distribution for the parent material, are plotted as histograms in Fig. 11. The turbidity current is strongly enriched in fines relative to the parent. This enrichment developed because the overriding current was unable to suspend sand at concentrations comparable to the source values. While the parent was composed of 52% mud, the lowermost sample from the current was 93% mud. All sizes of sand were found in this lowermost sample, but in reduced quantity. The sample from the second siphon recorded a substantial reduction in particle size (Fig. 11). Medium, coarse and very coarse sand were all absent at this position within the interior of the current. This abrupt reduction in grain size is consistent with sand being limited to the lower third of each current.

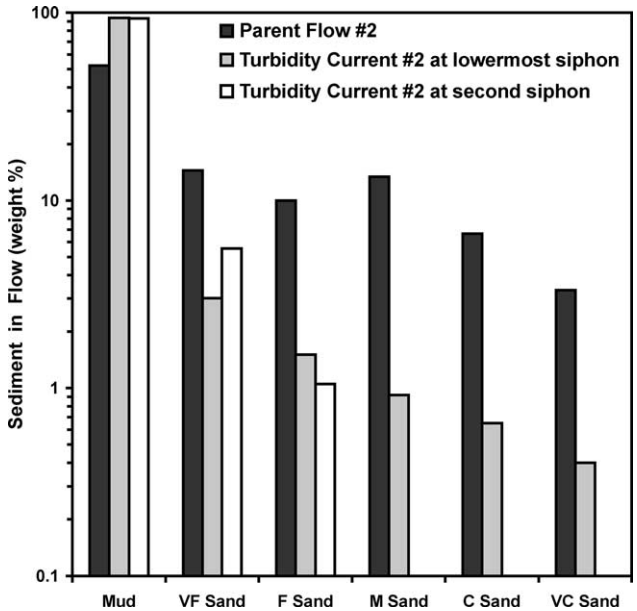

Fig. 11. Differences in grain size between the parent material and the overriding turbidity current for Run 2 (Table 1). Only samples collected by the two lowest siphons contained a measurable fraction of sand. The parent material is significantly coarser than the sample from the lowermost siphon, which is, in turn, significantly coarser than the sample from the second siphon. The vertical positions for these siphons are marked by the two triangles located at 0.12 and 0.14 m above the channel bed in Fig. 10. Samples collected from siphons at higher levels in the current consisted exclusively of mud (silt + clay-size particles).

6. Constructing an erosion equation for turbidity current production

Our observations of turbidity currents generated by the processes of grain plucking and shear-layer shedding from the heads of parent flows have led us to construct a conceptual framework within which the rate of sediment production via head erosion can be quantified. The framework is outlined diagrammatically in Fig. 12 and is described here by the following expression of mass conservation

$$R_h L_h \varepsilon_p T = (A_t \varepsilon_t) + (A_r \varepsilon_r) \quad (1)$$

where the volume of sediment lost from a parent flow per unit width is equal to the product of, R_h, the erosion rate of the head, L_h, the arc length for the section of head subject to erosion (i.e. the distance from the channel base to the point of flow separation), ε_p, the average value for sediment concentration (1-porosity) in the unmodified parent material and, T, some given interval of time. Sediment volume lost via erosion from the head of the parent flow is either added to the developing turbidity current or rapidly settles out onto the top of the parent flow and is effectively accreted to it. The volume of sediment present in the overriding turbidity current is equal to the product of the total volume for the turbidity current per unit width, A_t, and the average concentration for suspended sediment within the current, ε_t. The volume of sediment that is simply transferred from the head to the upper surface of a parent flow following a pathway of upward ejection and rapid settling is equal to the product of A_r, the volume of resedimented parent material per unit width and, ε_r, the average value for sediment concentration (1-porosity) in the resedimented parent material. By summing $(A_t \varepsilon_t)$ and $(A_r \varepsilon_r)$ all of the sediment eroded from the head either by grain plucking associated with strongly cohesive flows or by shear-layer shedding associated with some moderately coherent flows is fully accounted for and the erosion rate for a parent flow, R_h, can be unambiguously related to the suspended-sediment concentration in the turbidity current above, ε_t.

Our experimental technique was not set up to acquire direct measures of A_r and ε_r, so in determining the head erosion for Runs 1 and 2 we assumed that A_r was very small

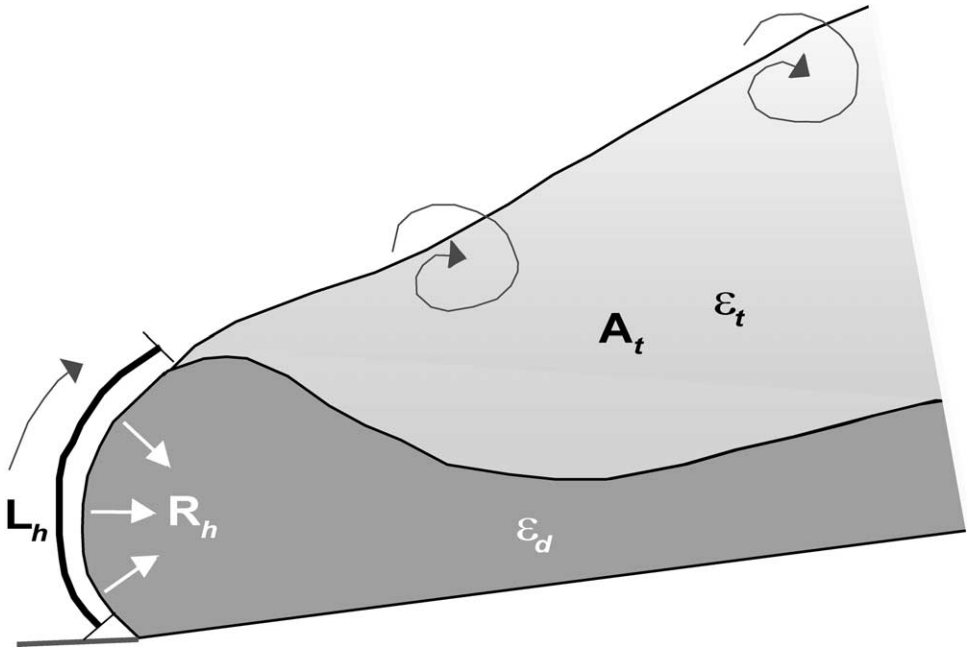

Fig. 12. A framework for quantifying the erosion rate of sediment, R_h, from the leading edge of a strongly coherent debris flow in two dimensions: L_h is the arc length for the debris head subject to erosion (i.e. the length from the bed to the point of flow separation); ε_d and ε_t are the average concentrations of sediment in the debris flow and the turbidity current, respectively; and A_t is the volume of turbidity current per unit width. R_h can be thought of as the velocity of erosion associated with the stripping away of layers of sediment from the head. Assuming all of this eroded sediment remains suspended in the turbidity current the conservation of sediment mass requires that $R_h = A_t\varepsilon_t/[L_h\varepsilon_d T]$ where T is some given length of time.

and neglected the sink term within the right-hand set of parentheses on the right-hand side of Eq. (1). After setting $(A_r\varepsilon_r) = 0$, Eq. (1) can be rearranged to solve for erosion rate using data collected from turbidity currents by the siphon rack and measurements of head dimensions from video. This simplified equation is

$$R_h = (A_t\varepsilon_t)/(L_h\varepsilon_p T) \quad (2)$$

Values of R_h for Runs 1 and 2 calculated using Eq. (2) are plotted in Fig. 13 as a function of head velocity, U_h, for the two parent flows (Table 1). We chose this parameter for two reasons. First, since the composition for the two runs is identical, U_h was the only independent parameter that varied between the two runs. Second, it allows us to compare the rate at which the head is moving through the system against the rate at which it is being eroded. The calculated values for head-erosion rate are about 460 and 240 times smaller than the measured down-slope velocities for parent flows 1 and 2, respectively. These very small values for erosion rate would become somewhat larger if we were able to properly account for the mass described by $(A_r\varepsilon_r)$. This term accounts for all of the material that is removed from the head of a parent flow, but is too massive to be suspended by and incorporated into the evolving turbidity current. Included are non-deforming chunks of parent material torn off of the leading edges of strongly coherent flows, as well as portions of thin layers shed from the heads of moderately coherent flows that did not fully disintegrate within turbidity currents before settling out onto flow tops. Also included are those individual sediment grains that were ejected into the water column, but were too large to be suspended within the overriding turbidity current. A qualitative feeling for the volume of material this represents for these particular runs can be gained through inspection of the grain-size data presented in Fig. 11. We interpret the relative paucity of sand in the turbidity current to indicate that almost one-half of the sediment removed from the heads was too massive to be suspended within the current and quickly settled out onto the upper surface of the parent flow. The inclusion of this sediment in the calculations would approximately double the estimated values for erosion rate presented in Fig. 13.

With only two data points (Fig. 13), we do not have enough information to develop a predictive equation for sediment erosion from the heads of parent flows. In spite of this deficiency, the small set of erosion data can be used to infer two likely components of the final erosion rule. First, the rate of head erosion appears to be very sensitive to head velocity. The head velocity for Run 2 was only 1.5 times larger than that for Run 1 (Table 1), but the determined erosion rate for Run 2 was 2.8 times greater than that for Run 1. This sensitivity is consistent with erosion being a function of shear stress, which scales with U_h^2. Second, the data support the inclusion of a critical shear stress for the parent material in any erosion equation. The trend line in Fig. 13 forecasts vanishingly small rates of erosion at head velocities less than roughly 0.1 m/s. The critical shear stress for this particular parent material would be therefore associated with a head velocity of approximately this magnitude. In short, our data appear consistent with a standard formulation of the erosion equation for cohesive

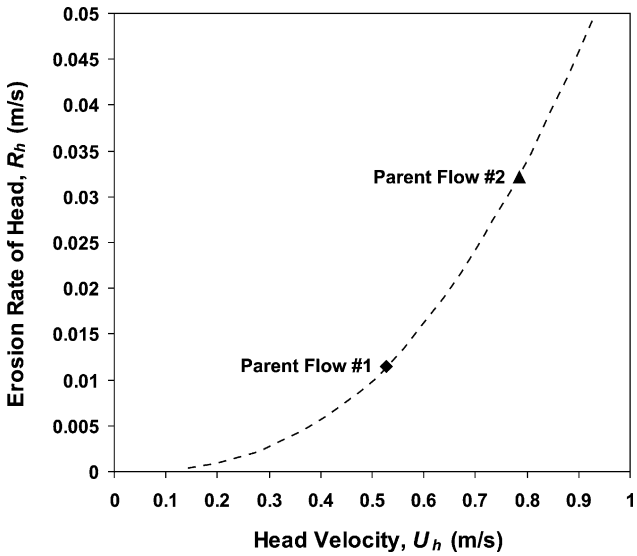

Fig. 13. Estimated values for the rates of sediment erosion from the heads of parent flows 1 and 2 (Table 1). These rates where calculated following mass-balance considerations as outlined in Fig. 12. Calculated values for τ_y/τ_f suggest that parent flow 1 was transitional between a strongly and moderately coherent head, while parent flow 2 was a moderately coherent head. The trend line defined as the best-fit power law is dashed in to highlight the sensitivity of turbidity current production to the down-slope velocity of its parent flow. This sensitivity is consistent with having the dynamic stresses that act on the head of a flow scale with the square of its velocity.

sediment (e.g. Equation (1) of Kuijper, Cornelisse, & Winterwerp, 1989).

7. Scaling

Our experiments were conducted at a scale that was much smaller than those of natural systems. It is therefore appropriate to discuss how our results can be extrapolated to natural flows while accounting for this difference in scale. We are particularly interested in exploring two issues: (1) how best to relate macroscopic properties for the flows (e.g. flow velocity, flow thickness, and bed slope) between natural and laboratory scales; and (2) how to relate compositional differences between parent mixtures prepared in the laboratory to those generated by the failure of pre-existing sedimentary deposits. These considerations of the parent flows and the parent mixtures are presented below.

7.1. Distorted scale modeling

We employ a distorted geometric scaling when comparing natural (prototype) flows to our experimental (model) flows. This technique involves the scaling down of the vertical and horizontal dimension for the system by differing amounts; thereby allowing us to compare the thin parent flows moving on steep slopes in the laboratory against the thick natural flows that traverse shallower slopes. The vertical scale ratio λ_v is any vertical length in the model divided by the corresponding vertical length in the prototype, and the horizontal scale ratio λ_h is any horizontal length in the model divided by the corresponding horizontal length in the prototype. Dynamic similarity between the prototype and model flows is maintained if the values for each of the dimensionless parameters necessary to characterize their dynamics are held constant. Identification of the appropriate dimensionless parameters for characterizing granular mass flows can be difficult (Iverson, 1997). A discussion of the processes that can complicate mass-flow rheology, as they apply to experimental subaqueous flows, can be found in Marr et al. (2001) and Mohrig et al. (1998). Here we consider only the narrowly defined case of subaqueous debris flows with a Bingham (visco-plastic) rheology. For this particular case similarity of bulk flow properties requires equality in four dimensionless numbers. These numbers are the densimetric Froude number, Fr, the Reynolds number, Re, the dimensionless yield strength, τ_y^*, and the relative density, ϕ,

$$\phi = \rho_d/\rho_w \tag{3}$$

$$\tau_y^* = \tau_y/\rho_d U^2 \tag{4}$$

$$Re = UH/\nu_d \tag{5}$$

$$Fr = U/\sqrt{(\phi - 1)gH} \tag{6}$$

where U is flow velocity, H is flow thickness, ν_d is the kinematic viscosity of the parent material, and ρ_d and ρ_w are the densities for the parent material (sediment + water) and the ambient fluid (water), respectively. In the analysis below we assume that the values of ρ_d and ρ_w are the same in the model and the prototype, ensuring similarity in ϕ.

Applying the principles of distorted modeling (Graf, 1971) yields the following scalings

$$(L_r)_m = \lambda_h (L_r)_p \tag{7}$$

$$(H)_m = \lambda_v (H)_p \tag{8}$$

$$(S)_m = \lambda_v/\lambda_h (S)_p \tag{9}$$

$$(U)_m = \lambda_v^{1/2} (U)_p \tag{10}$$

$$(\tau_y)_m = \lambda_v (\tau_y)_p \tag{11}$$

where L_r is the runout length for the flow, S is bed slope, and the subscripts m and p denote the model and prototype, respectively. These relationships provide an estimate as to how our experiments might be extrapolated to natural scale assuming $\lambda_v = 1/100$ and $\lambda_h = 1/500$. Representative model values for L_r, S, H, U, and τ_y from the experiments of Mohrig et al. (1998) and Marr et al. (2001) are 7.0 m, 5°, 5.0×10^{-2} m, 6.0×10^{-1} m/s, and 30 Pa, respectively. These model values render the respective prototype values of 3.5×10^3 m, 1°, 5.0 m, 6.0 m/s, and 3.0×10^3 Pa. These prototype values are comparable to estimated values for a variety of natural flows (e.g. Hampton et al., 1996).

The success with which any one of the experimental flows can be approximated by the Bingham rheology partly

depends on the degree to which the liquid and solid phases of the original parent mixture separate from each other during transport down the channel. For all strongly coherent and most moderately coherent flows this segregation was very small and the Bingham approximation is considered a suitably accurate description of their flow behaviors. This assumption is quantitatively supported by the measurements of Parsons et al. (2001) on subaerial debris flows with similar compositions. However, suitability of the Bingham approximation breaks down as the separation between the two phases increases during transport. Because of this our weakly coherent flows may have deviated sufficiently from the Bingham rheology that a different scaling is required (Iverson, 1997). While the collection of data necessary to develop this scaling was beyond the scope of this project, observing the effects of change in parent-flow rheology on turbidity-current production was not. The consequences of a changing parent flow on the production of an affiliated turbidity current are outlined below.

7.2. Pore-pressure dissipation and the unmixing of parent flows

The successful failure of most undrained sedimentary deposits involves a collapse in the pre-existing structure to the grain framework (Hampton et al., 1996; Iverson, 1997). This contraction in the grain framework causes pore-fluid pressure build-up, as part of the vertical normal stress for the mixture is transferred from the framework onto the pore water itself. These positive excess pore pressures can approach lithostatic values and when they do, they effectively lubricate the flows by reducing their internal friction (Norem, Locat, & Schieldrop, 1990; Major & Iverson, 1999). Dissipation of the excess pressures requires the unmixing of original parent mixtures. In other words, the liquid phase must separate from the solid phase. Iverson (1997) proposed that the characteristic timescale for pore pressure decay, t_{dif}, is equal to

$$t_{dif} = H^2 \mu / kE \tag{12}$$

where μ is the dynamic viscosity of pore fluid with suspended fine sediment, k is the hydraulic permeability of the mixture, and E is the stiffness of the mixture. How large or small the calculated value for the timescale is relative to the duration of an experimental flow determines whether the parent material traverses the laboratory tank with minor modification to its original composition or whether substantial unmixing occurs, modifying the rheology of the dense flow as it moves down slope.

The calculated values of t_{dif} for Runs 1 and 2 (Table 1) were more than an order of magnitude greater than the lengths of time taken by these flows to traverse the flume (Mohrig et al., 1998). Insufficient time for excess pore pressures to dissipate from the parent mixture meant that upward-moving pore fluids contributed insignificant volumes of sediment to the overlying turbidity currents. The methods of turbidity-current production we have presented up to this point include no component of a *fluidization transformation* as described by Fisher (1983). Flows undergoing this transformation segregate vertically into a laminar underlying layer and a turbulent overriding layer. Turbidity currents developing via this process are predominantly composed of particles elutriated from the original parent mixtures by upward-moving pore fluids. Postma et al. (1988) have studied turbidity currents generated by fluidization transformations. Their experiments provide an excellent illustration as to the consequences of rapid unmixing of the liquid and solid phases constituting the parent mixture. In their runs the coarser sand and gravel settled down through and segregated from the fluid and its suspended sediment within the first 1.3 m of transport down the flume. This upward-directed loss of fluid + fines from the original mixture resulted in a substantial increase in the value of intergranular friction for the remainder of the dense flow. In spite of this increase in the internal friction, these sediment-charged flows continued to move down the flume because the slope of the bed was high enough, 25°, to overcome the resisting forces.

Deposits of natural flows where t_{dif} is interpreted as small relative to the transport times for the evolving parent flows have been reported by Falk and Dorsey (1998), Mutti et al. (2000), and Sohn (2000), among others. All of these cases involve relatively coarse-grained original failures and we assume that the relatively small values for t_{dif} were the products of high permeabilities for the coarse-grained mixtures (Eq. (12)). In cases studied by Falk and Dorsey (1998) and Sohn (2000) the elutriation of fine sediment from the original mixtures is a likely cause for the mobility of residuum flows being restricted to the foresets of deltas. These were the only locations where bed slopes were sufficiently large so that the body forces exceeded the resisting forces associated with intergranular friction. This meant that turbidity currents generated from these fluidization transformations developed over distances no greater than the breadths of the steep delta foresets. For the events interpreted by Falk and Dorsey (1998) this distance was less than 20 m. Such a short distance stands in contrast to those distances over which turbidity currents are produced by headward sediment erosion or by surface transformations. For example, Masson (1996) and Souquet, Eschard, and Lods (1987) describe modern and ancient turbidites generated from parent flows that traveled many tens of kilometers from their points of initiation. Processes measured in our laboratory runs are consistent with turbidity-current development during extended transport.

8. Discussion

Studies of seascape evolution have traditionally gone no further than to relate the occurrence of the sculpting

turbidity currents to either relative lowstands in sea level (e.g. Van Wagoner, Mitchum, Campion, & Rahmanian, 1990) or to specific triggering mechanisms (i.e. earthquakes, storms and floods; Hampton et al., 1996; Normark & Piper, 1991). While these conditions are necessary to set up the currents, they alone cannot predict any of the governing characteristics for the currents such as their initial volume, velocity, and sediment concentration. Relating an impulsive trigger to a specific current requires information regarding the processes of sediment transference from a pre-existing shelf-edge or slope deposit to a relatively dilute turbidity current. A goal of the experiments presented here was to establish a quantitative framework for characterizing turbidity-current production so as to benefit models of submarine landscape development.

Three mechanisms for producing turbidity currents from parent mass flows were studied in the laboratory. The first two simply involved the erosion of material from the head of the parent flow and its ejection into the overlying column of water where it could be worked into a developing turbidity current. The third involved a more direct transformation of the parent flow to a turbidity current via the production of turbulence within the head of the parent flow. All three styles of transference from the original flow to a turbidity current were focused at the very fronts or heads of the parent debris flows because this is where large dynamic stresses developed as the standing water (i.e. ambient fluid) was accelerated by the flows out of their paths. Our laboratory measurements confirm that the influence of these stresses on turbidity-current development depends on their magnitude relative to an effective yield strength for the parent mixture of sediment and water. Data from Marr et al. (2001) and Mohrig et al. (1998) were used to constrain the critical values for a ratio of yield strength to dynamic stress, τ_y/τ_f, at which changes in character of the transfer processes were observed.

Grain-by-grain erosion from the leading edge of the parent flow was the only active process observed at values for $\tau_y/\tau_f > 0.2$. At values for $\tau_y/\tau_f \leq 0.2$ the dynamic stresses were sufficiently large to instigate the local development of shearing parent material on the surfaces of the heads of flows. As long as the internal deformation within the shearing layer was laminar, the layer remained as a relatively thin veneer on the moving head. This was mostly due to the fact that material was continually being swept backward and detached from the heads of flows. Ejected into the overlying water column, many of these thin layers disintegrated within the developing turbidity currents. A critical value of τ_y/τ_f for the onset of turbulence within the heads of parent flows was not well constrained by the experiments. This is mostly due to the small number of measured flows that underwent this transformation. Presently we can only propose that this transition is associated with values for τ_y/τ_f only somewhat smaller than the critical value of 0.2. Future work is required to better define the local conditions associated with the laminar–turbulent transition within the heads of parent flows themselves. Additional work is also needed to obtain a more accurate characterization for the dynamic stresses driving the transference of sediment. The use here of the stagnation or dynamic pressure as a scale value for these stresses is considered only a first step in quantifying the environmental conditions at the heads of parent flows that govern the character of turbidity-current development.

Data such as those presented in Figs. 10, 11 and 13 represent only a first step toward building a predictive model of turbidity current production via the erosion of sediment from submarine debris flows and slides. A geometric and kinematic framework for the model is presented in Fig. 12. We envision the dynamical component of this model possessing descriptions for a number of basic processes that include: (1) an algorithm relating the boundary conditions for the system (e.g. long profile, original failure volume) and the parent-material composition to the forward velocity and thickness of the flow; (2) an algorithm relating the velocity and shape for the head of the flow to the dynamic stresses that act on it; (3) an equation relating the magnitude of these dynamic stresses to the rate and style at which the head is eroded; and (4) an algorithm describing the efficiency with which the evolving turbidity current incorporates all of the sediment shed from the head of the parent flow. This framework is constructed assuming that the leading edge of any parent flow can be treated as a discrete surface. The formulation breaks down for the case in which the head of a flow becomes turbulent. In this case the interface separating clear water from the parent material cannot be adequately approximated by a single surface. The turbulent mixing of clear water into the head requires that a zone with finite thickness and a spatially varying sediment concentration replace the model surface. Additional work is required to characterize both the structure of and the trends in these transformations.

The acoustical imaging of parent flows in the laboratory (Fig. 9) clearly shows that any production of turbulence within the parent material is focused at their heads. Data collected by Marr (1999) suggests that the mixing length increases, moving backward from head, as the coherency of the parent flow drops. Under what conditions might an entire parent flow become turbulent? A partial answer to this question is found in experimental results of Van Kessel and Kranenburg (1996) describing the motion of fluid mud on an inclined subaqueous bed. The model fluid mud consisted of china clay suspended within tap water. Whether a fluid mud traveled down the sloping bed as a laminar or turbulent flow depended on the concentration of china clay in the original mixture. In their experiments only those flows with less than 10% sediment (clay) by volume (>90% water) were fully turbulent. Flows with >10% sediment by volume (<90% water) were laminar with a distinct interface separating

the fluid mud from an overriding turbidity current. The Van Kessel and Kranenburg (1996) experiments suggest that very low sediment concentrations are required in order for the effective viscosities and strengths of remobilized deposits to be sufficiently small to ensure fully turbulent flow. We suspect that these conditions occur seldom in sandy shelf-edge or upper continental slope deposits. The higher sediment concentrations that are prerequisite for building the grain frameworks that can support the weight of sand and silt-size particles would most likely result in flowing material that did not pass through the laminar–turbulent transition. For these reasons we propose that any turbulent–laminar transition occurring within sandy natural flows would be focused at their heads, as seen in the laboratory experiments described here.

Measurements of suspended sediment for the turbidity currents produced by Runs 1 and 2 revealed that less than 1% of the sediment that makes up the parent flow is transferred to the overriding current (Fig. 10; Table 1). These small values of exchange indicate the relative inefficiency of sediment erosion from the heads of slides and debris flows as a production mechanism. A great deal of this inefficiency is a consequence of the very small fraction of the total surface area of the parent flow that is acted on by erosional processes. The generation of currents by turbulent mixing at the fronts of some parent flows was observed to be a more efficient, but not yet quantified, process. Even in these cases the net transfer of sediment from the parent to the turbidity current may be small because the process is limited to a small fraction of the total volume of parent material available for transformation (Fig. 9). It is our intention that the laboratory results presented here will contribute to continuing work on the processes affecting turbidity-current production so as to improve the quantitative predictability of initial conditions for currents generated from impulsive failures of continental shelf and slope deposits.

Acknowledgements

Support for our research was provided in part by the Marine Geology and Geophysics program (STRATAFORM project N/N00014-93-1-0300) of the US Office of Naval Research, Mobil Technology Company (1996–1998), and the STC Program of the National Science Foundation under Agreement Number EAR-0120914. We thank Gary Parker, Chris Ellis and Kelin Whipple for helping develop the experimental technique and Peter Harff for his assistance in performing the experiments. This project also benefited from thoughtful discussions with Chris Paola and G. Shanmugam. T. Hickson and R. Tinterri provided very constructive reviews of this manuscript.

References

Allen, J. R. L. (1971). Mixing at turbidity current heads, and its geological implications. *Journal of Sedimentary Petrology*, *41*, 97–113.

Falk, P. D., & Dorsey, R. J. (1998). Rapid development of gravely high-density turbidity currents in marine Gilbert-type fan deltas, Loreto Basin, Baja California Sur, Mexico. *Sedimentology*, *45*, 331–349.

Federal Interagency Sedimentation Project (1941). *Laboratory investigation of suspended-sediment samplers*. Interagency Report 5 (99pp). Iowa City: Iowa University Hydraulics Laboratory.

Fisher, R. V. (1983). Flow transformations in sediment gravity flows. *Geology*, *11*, 273–274.

Graf, W. H. (1971). *Hydraulics of sediment transport*. New York: McGraw-Hill, 513pp.

Hallworth, M. A., Phillips, J. C., Huppert, H. E., & Sparks, R. S. J. (1993). Entrainment in turbulent gravity currents. *Nature*, *362*, 829–831.

Hampton, M. A. (1972). The role of subaqueous debris flows in generating turbidity currents. *Journal of Sedimentary Petrology*, *42*, 775–793.

Hampton, M. A., Lee, H. J., & Locat, J. (1996). Submarine landslides. *Reviews of Geophysics*, *34*, 33–59.

Hanks, R. W. (1963). The laminar-turbulent transition for fluids with a yield stress. *AIChE Journal*, *9*, 306–309.

Iverson, R. M. (1997). The physics of debris flows. *Reviews of Geophysics*, *35*, 245–296.

Kuijper, C., Cornelisse, J. M., & Winterwerp, J. C. (1989). Research on erosive properties of cohesive sediments. *Journal of Geophysical Research*, *94*(C10), 14341–14350.

Liu, K. F., & Mei, C. C. (1990). Approximate equations for the slow spreading of a thin sheet of Bingham plastic fluid. *Physics of Fluids*, *A2*(1), 30–36.

Major, J. J., & Iverson, R. M. (1999). Debris-flow deposition: effects of pore-fluid pressure and friction concentrated at flow margins. *Geological Society of America Bulletin*, *111*, 1424–1434.

Marr, J. G. (1999). *Experiments on subaqueous sand gravity flows: flow dynamics and deposit structure* (121pp). MS Thesis, University of Minnesota, Minneapolis.

Marr, J. G., Harff, P. A., Shanmugam, G., & Parker, G. (2001). Experiments on subaqueous sandy gravity flows: the role of clay and water content in flow dynamics and depositional structures. *Geological Society of America Bulletin*, *113*, 1377–1386.

Masson, D. G. (1996). Catastrophic collapse of the volcanic island of Hierro 15 ka ago and the history of landslides in the Canary Islands. *Geology*, *24*, 231–234.

Mohrig, D., Elverhøi, A., & Parker, G. (1999). Experiments on the relative mobility of muddy subaqueous and subaerial debris flows, and their capacity to remobilize antecedent deposits. *Marine Geology*, *154*, 117–129.

Mohrig, D., Whipple, K. X., Hondzo, M., Ellis, C., & Parker, G. (1998). Hydroplaning of subaqueous debris flows. *Geological Society of America Bulletin*, *110*, 387–394.

Morgenstern, N. R. (1967). Submarine slumping and the initiation of turbidity currents. In A. F. Richards (Ed.), *Marine geotechnique* (pp. 189–220). Champaign, IL: University of Illinois Press.

Mulder, T., & Syvitski, J. P. M. (1995). Turbidity currents generated at river mouths during exceptional discharges to the worlds oceans. *Journal of Geology*, *103*, 285–299.

Mutti, E., Tinterri, R., Di Biase, D., Fava, L., Mavilla, N., Angella, S., & Calabrese, L. (2000). Delta-front facies associations of ancient flood-dominated fluvio-deltaic systems. *Revista de la Sociedad Geologica de Espana*, *13*, 165–190.

Norem, H., Locat, J., & Schieldrop, B. (1990). An approach to the physics and the modeling of submarine flowslides. *Marine Geotechnology*, *9*, 93–111.

Normark, W. R., & Piper, D. J. W. (1991). Initiation processes and flow evolution of turbidity currents; implications for the depositional record.

In R. H. Osborne (Ed.), *From shoreline to abyss; contributions in marine geology in honor of Francis Parker Shepard* (pp. 207–230). *SEPM Special Publication 46*.

Parsons, J. D., Whipple, K. X., & Simoni, A. (2001). Experimental study of the grain-flow, fluid mud transition in debris flows. *Journal of Geology*, *109*, 427–447.

Postma, G., Nemec, W., & Kleinspehn, K. L. (1988). Large floating clasts in turbidites: a mechanism for their emplacement. *Sedimentary Geology*, *58*, 47–61.

Shanmugam, G. (2000). 50 years of the turbidite paradigm (1950s–1990s): deep-water processes and facies models—a critical perspective. *Marine and Petroleum Geology*, *17*, 285–342.

Sohn, Y. K. (2000). Depositional processes of submarine debris flows in the Miocene fan deltas, Pohang Basin, SE Korea with special reference to flow transformation. *Journal of Sedimentary Research*, *70*, 491–503.

Souquet, P., Eschard, R., & Lods, H. (1987). Facies sequences in large-volume debris- and turbidity-flow deposits from the Pyrenees (Cretaceous; France, Spain). *Geo-Marine Letters*, *7*, 83–90.

Thomas, D. G. (1965). Transport characteristics of suspension: VII. A note on the viscosity of newtonian suspensions of uniform spherical particles. *Journal of Colloid Science*, *20*, 267–277.

Van den Berg, J. H., Van Gelder, A., & Mastbergen, D. R. (2002). The importance of breaching as a mechanism of subaqueous slope failure in fine sand. *Sedimentology*, *49*, 81–95.

Van Kessel, T., & Kranenburg, C. (1996). Gravity current of fluid mud on sloping bed. *Journal of Hydraulic Engineering*, *122*, 710–717.

Van Wagoner, J. C., Mitchum, R. M., Campion, K. M., & Rahmanian, V. D. (1990). Siliciclastic sequence stratigraphy in well logs, cores, and outcrops: concepts for high-resolution correlation of time and facies. *AAPG Methods in Exploration Series*, *7*; 55pp.